

A. Huber, R. A. Pitts, A. Loarte, V. Philipps, P. Andrew, G. Arnoux, S. Brezinsek,
P. Coad, J.C. Fuchs, W. Fundamenski, S. Jachmich, A. Korotkov, G.F. Matthews,
K. McCormick, Ph. Mertens, J. Rapp, G. Sergienko, M. Stamp
and JET EFDA contributors

Plasma Radiation during Transient Events in JET

"This document is intended for publication in the open literature. It is made available on the understanding that it may not be further circulated and extracts or references may not be published prior to publication of the original when applicable, or without the consent of the Publications Officer, EFDA, Culham Science Centre, Abingdon, Oxon, OX14 3DB, UK."

"Enquiries about Copyright and reproduction should be addressed to the Publications Officer, EFDA, Culham Science Centre, Abingdon, Oxon, OX14 3DB, UK."

Plasma Radiation during Transient Events in JET

A. Huber¹, R. A. Pitts², A. Loarte³, V. Philipps¹, P. Andrew⁴, G. Arnoux⁴,
S. Brezinsek¹, P. Coad⁴, J.C. Fuchs⁵, W. Fundamenski⁴, S. Jachmich⁶, A. Korotkov⁴,
G.F. Matthews⁴, K. McCormick⁵, Ph. Mertens¹, J. Rapp¹, G. Sergienko¹, M. Stamp⁴
and JET EFDA contributors*

JET-EFDA, Culham Science Centre, OX14 3DB, Abingdon, UK

¹*Institut für Plasmaphysik IEF-4, Forschungszentrum Jülich GmbH, EURATOM Association,
Trilateral Euregio Cluster, D-52425 Jülich, Germany*

²*CRPP, Association EURATOM-Confederation Suisse, EPFL, Lausanne, Switzerland*

³*EFDA Close Support Unit – Garching, Boltzmannstrasse 2, D-85748 Garching, Germany*

⁴*Euratom/UKAEA Fusion Association, Culham Science Centre, Abingdon, Oxon OX14 3DB, UK*

⁵*Max-Planck-Institut für Plasmaphysik, EURATOM Association, 85748 Garching, Germany*

** See annex of M.L. Watkins et al, “Overview of JET Results”,
(Proc. 21st IAEA Fusion Energy Conference, Chengdu, China (2006)).*

Preprint of Paper to be submitted for publication in Proceedings of the
35th EPS Conference on Plasma Physics, Hersonissos, Crete, Greece
(9th June 2008 - 13th June 2008)

INTRODUCTION.

In the future ITER tokamak, the Plasma-Facing Components (PFCs) will be subject to large power loads during intense transient events such as disruptions, VDEs, MARFEs and bursts of Edge Localised Modes (ELMs). During JET plasma disruptions, the thermal energy ($\leq 10\text{MJ}$) and magnetic energy ($\leq 20\text{MJ}$) are lost in form of heat to the plasma-facing components on timescales of less than 1ms and 20ms [1], respectively. Initially, the thermal energy is dissipated in the thermal quench followed by the magnetic energy dissipation in the current quench. During the current quench phase, the energy stored in the poloidal magnetic field is radiated non-uniformly over the first wall surfaces and may significantly contribute to the local power loads onto PFCs. The ELM radiation behaviour has been analysed in detail in the Type I ELMy H-mode regime which is the baseline scenario for operation of ITER in high fusion gains. In present tokamaks, the plasma energy drop normalised to the pedestal energy, $\Delta W_{\text{ELM}}/W_{\text{ped}}$ is typically 3-10% during a Type I ELM.

A significant part of this energy can be found in form of plasma radiation, located mostly in the divertor region (in the present contribution, it is integrated over $\sim 2\text{ms}$, which is considerably longer than the ELM target power deposition of several $100\mu\text{s}$).

EXPERIMENTAL SET-UP

The JET bolometer camera system has recently been substantially upgraded, allowing significantly improved spatial and temporal resolution of the radiation distribution, particularly in the divertor region [2]. This allows a greatly improved tomographic reconstruction of the radiation pattern on a timescale of the order of the typical duration of a Type I ELM cycle ($\sim 1\text{ms}$). The tomographic reconstruction model (anisotropic diffusion model) has been coupled with a Monte-Carlo technique to calculate the poloidal radiation distribution, hence the radiation load onto the vessel, during these transient events.

RESULTS AND DISCUSSION

The important events which are dangerous for plasma-facing components are the power loads onto the wall during disruptions, MARFEs and VDEs. The energy loss in disruptions can be divided into two phases as shown in Fig.1: first the thermal energy is lost to the walls in the thermal quench. This is followed by the loss, in the current quench, of the energy stored in the poloidal magnetic field. The energy balance studies of the JET disruptions [3] have indicated that the magnetic energy (E_{mag}) transferred to the plasma by Ohmic heating in the current quench is mostly radiated to the first wall ($E_{\text{rad}} \approx E_{\text{mag}}$).

The tomographic reconstruction model which is used (anisotropic diffusion model) has been coupled with a Monte-Carlo technique to calculate the poloidal radiation distribution, hence the radiation load onto the vessel, during these transient events. It is found that the radiation distribution is strongly poloidally asymmetric in particular in the current quench as shown in Fig.1. Figure 2 shows the evaluated radiation peaking factors (the local radiation power load onto the wall normalised

to its value averaged over the entire surface) as function of the poloidal distance along the wall for two types of disruptions (density limit disruption already discussed in Fig.1 and disruption driven by Neoclassical Tearing Mode (NTM)). A maximum of the observed radiation peaking factor for the disruption current quench of about 2.5 is observed. It is located at the inner main chamber wall. These “peaking factors” have been used to extrapolate to ITER reference conditions. With the poloidal magnetic energy of ITER of $E_{\text{mag}} \sim 600\text{MJ}$ and a current quench time of $\sim 36\text{ms}$ [4], a maximum radiative load of 61MW/m^2 is obtained (with assumption $E_{\text{rad}} \approx E_{\text{mag}}$) using a radiation peaking factor of 2.5. This type of radiation losses (for the current quench alone) may increase the beryllium temperature to about half the melting point.

For MARFEs investigation, L-mode density limit experiments have been performed with $B_T = 2.4\text{T}$, $I_p = 1.7\text{MA}$ in ohmic discharges and in discharges with additional NBI-power of 1.0-1.8MW. The plasma density was raised steadily to the density limit by gas fuelling into the inner divertor. With continuous deuterium puffing, a high density, low temperature plasma forms inside the separatrix near the X-point. This is the so-called X-point MARFE (XPM). Figure 3 shows the tomographic reconstruction of radiation in the divertor region at three different \bar{n}_e . $2.56 \times 10^{19} \text{ m}^{-3}$. The outer divertor at this time is partially detached. $3.0 \times 10^{19} \text{ m}^{-3}$ and $3.37 \times 10^{19} \text{ m}^{-3}$. The radiation moves entirely to the X-point, forming an XPM at 80% radiative power fraction. The outer divertor at this time is fully detached. A maximum of the observed radiation peaking factor for MARFEs is of about 4.5. The radiation peaking occurs at the outer divertor target during the X-Point MARFE. With the fusion power of ITER of $\sim 400\text{MW}$ and a radiation fraction of 80-100%, a maximum radiative load of 0.7MW/m^2 is obtained using a radiation peaking factor of 4.5. The VDE disruption generates the largest heat loads. Figure 4 shows radiation peaking factors before VDE and during current quench phase of the VDE disruption. A maximum of the observed radiation peaking factor for the VDE-disruption current quench of about 5 is observed. With the poloidal magnetic energy of ITER of $\sim 600\text{MJ}$ and a current quench time of $\sim 36\text{ms}$, a maximum radiative load of 123MW/m^2 is obtained using a radiation peaking factor of 5. The ‘ablation/melting parameter’ [5], which determines the surface temperature rise caused by VDE, can reach values $23\text{MJ m}^{-2} \text{ s}^{-1/2}$ that exceed the value required for beryllium melting ($20\text{MJ m}^{-2} \text{ s}^{-1/2}$).

Dedicated experiments aiming at the characterisation of transient loads during large Type I ELMs have been performed during the 2007 JET campaigns at high plasma current and input power: $I_p = 3.0\text{MA}$, $B_T = 3.0\text{T}$, $q_{95} = 3.2$, $\delta_u \sim 0.22$, $\delta_l \sim 0.28$, $k = 1.73$, 19MW NBI and 1.4MW ICRH power. The gas fuelling has been varied in a series of repeated ELMy H-mode 3.0MA discharges with strike points located on the lower vertical tiles of the MkII-HD divertor to produce Type I ELMs of different sizes ($\Delta W_{\text{ELM}}/W_{\text{ped}}$ increases with decreasing gas fuelling) in the ELM energy range $\Delta W_{\text{ELM}} = 0.2 \rightarrow 0.9\text{MJ}$.

Discharges without gas fuel show large (giant) ELMs with $\Delta W_{\text{ELM}} \approx 0.9\text{MJ}$. Figure 5 presents the dependence on ΔW_{ELM} of the radiated plasma energy following the ELM crash. Here the radiated energy contains only the part of the radiated losses which occurs during the first main peak during

the ELM. For an ELM energy below 700kJ (roughly), the radiated plasma energy is proportional to the ELM energy, as expected from the observed linear correlation between impurity influxes and ELM sizes. In this range the ELMs radiates ~50% of the ELM energy drop. Beyond a ΔW_{ELM} of ~700kJ, a non-linear increase of the divertor radiation occurs which is interpreted as an indication of additional carbon ejection from the target tiles, possibly due to ablation of the co-deposited layers in the inner divertor [6]. The ELM-induced radiation is always higher at the inner than at the outer divertor with the asymmetry increasing approximately linearly up to a total \hat{w}_{ELM} of about 0.6 MJ and decreasing for higher ΔW_{ELM} .

SUMMARY AND CONCLUSION

The radiation distribution during transient events is poloidally asymmetric with the radiation peaking at the inner main chamber wall during the current quench in density limit and NTM-driven disruptions. During the X-Point MARFE the radiation peaking occurs at the outer divertor target during the X-Point MARFE. Maximum of the observed “radiation peaking factor” for the disruptive current quench is less than 3 and for MARFEs of about 4.5, and of about 5 during VDEs. Radiation losses during VDEs (for the current quench alone) will increase the Be temperature to values around the melting point.

The ELM radiation behaviour has been analysed in detail in the Type I ELMy H-mode regime which is the baseline scenario for operation of ITER in high fusion gains. A significant part of the total ELM energy loss can be found in form of plasma radiation, located mostly in the divertor region. Large Type I ELMs with energy losses above 0.7MJ show enhanced radiation losses, which are associated with the ablation of carbon layers in the inner divertor. The ELM-induced radiation is always higher at the inner than at the outer divertor with the asymmetry increasing approximately linearly up to a total ΔW_{ELM} of about 0.6MJ and decreasing for higher ΔW_{ELM} .

ACKNOWLEDGEMENT

This work, supported by the European Communities under the contract of Association between EURATOM and FZJ, was carried out within the framework of the European Fusion Development Agreement. The views and opinions expressed herein do not necessarily reflect those of the European Commission.

REFERENCES

- [1]. V. Riccardo et al., Nucl. Fusion **45** (2005) 1427.
- [2]. A. Huber, K. McCormick, P. Andrew, et al., Fusion Eng. Design **82** (2007) 1327,
- [3]. J.I. Paley et al., J. Nucl. Mater. **337-339** (2005) 702.
- [4]. J.C. Wesley et al., 2006 IAEA Fusion Energy Conf (Chengdu, China), paper IT/P1-21
- [5]. G. Federichi et al., J. Nucl. Mater. **313-316** (2005) 11.
- [6]. A. Huber et al., submitted to J. Nucl. Mater.

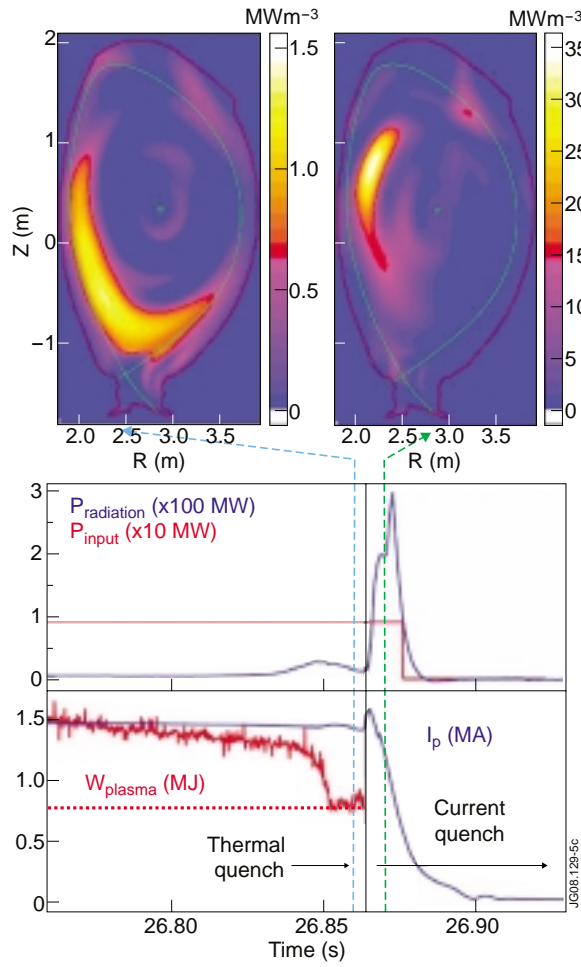


Figure 1: Radiation distribution during the disruption.

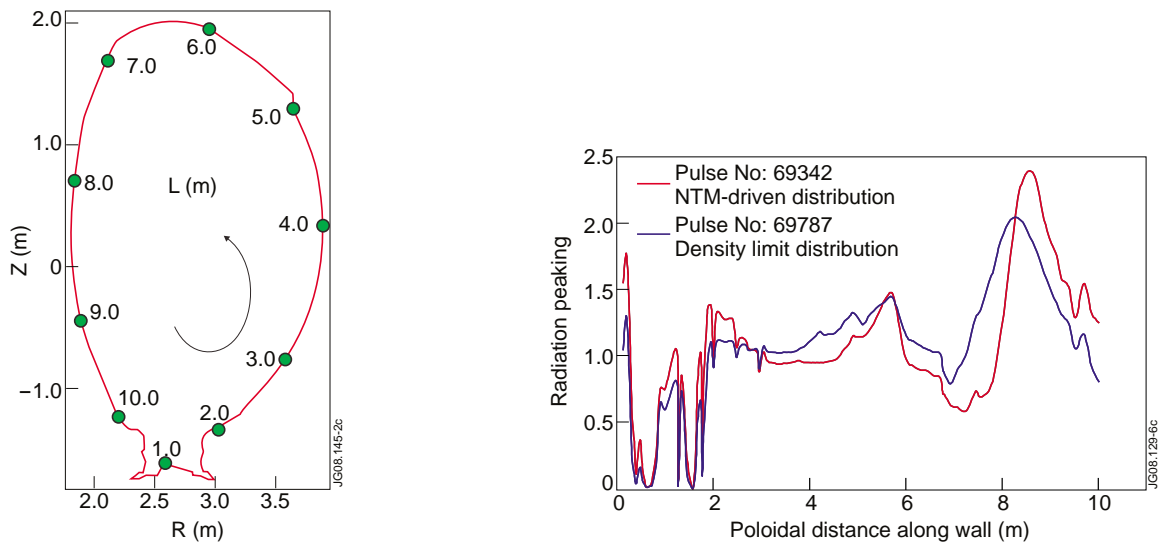


Figure 2: Radiation peaking factors during the current quench in JET.

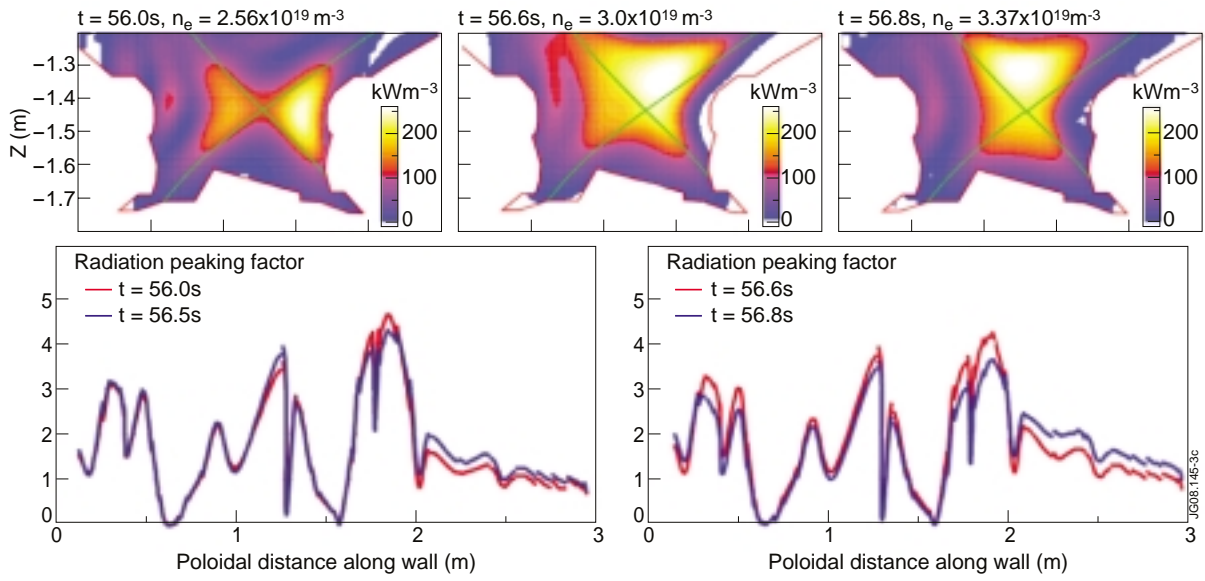


Figure 3: Tomographic reconstruction of the total radiation and the radiation peaking factors in the divertor region at different \bar{n}_e .

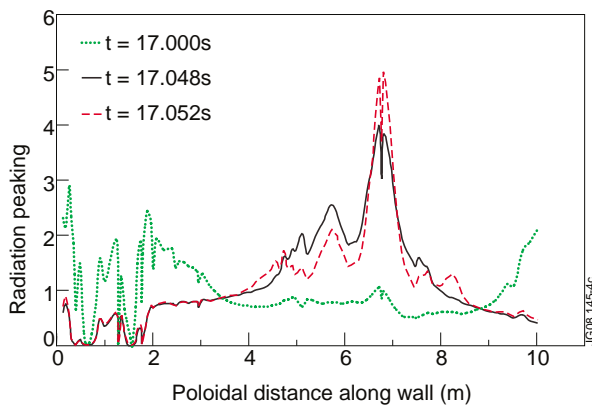


Figure 4: The radiation peaking factors before VDE (red) and during the current quench phase of the VDE disruption.

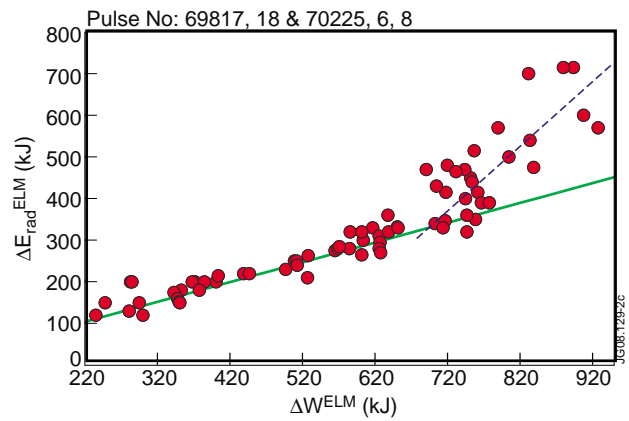


Figure 5: Radiated Plasma energy following Type I ELMs versus ELM energy loss.